Analysis of Deflection Effect of 2024 YR4 Asteroid Under the Velocity Increment Deviation of Kinetic Impact

YANG Xiaomin[1]，ZHANG Jianying[2]，ZHANG Feng[2]，LI Xiangyu[1]

（1. School of Aerospace Engineering, Beijing Institute of Technology, Beijing 100081, China；
2. China Academy of Launch Vehicle Technology, Beijing 100076, China）

Abstract：Focusing on the defense against kinetic impact of the near-Earth asteroid 2024 YR4, the effect of orbital deflection under velocity increment deviation was investigated. Firstly, an orbital evolution model integrating planetary perturbations and impact errors was established. Secondly, the influence of velocity increment error on the orbital deflection effect of the asteroid was systematically analyzed by the semi-analytical method of State Transition Tensor (STT). Finally, the differences in the evolution of the major axis of the error ellipsoid after impact at different times were analyzed. The study found that the evolution of orbital uncertainty caused by initial velocity increment error was dominated by the orbital phase, and the magnitude of the velocity increment only affected the error amplitude rather than the propagation form. When impacts were implemented at different initial moments and evolved for the same duration, the difference in the size of the major axis of the error ellipsoid reached 3.7 times, indicating that the timing of the impact had a significant impact on the uncertainty of the orbital deflection effect. In addition, the analysis found that the Earth Star rendezvous event in 2028 will alter the expected deflection. This study provides reference for developing asteroid defense strategies that consider error propagation.

Keywords：uncertainty；asteroid；kinetic impact；state transition tensor

Highlights：

- A high-precision orbital evolution model for near-Earth asteroid 2024 YR4 is established.
- The actual orbital deflection distance of 2024 YR4 is found to deviate from theoretical predictions due to gravitational perturbations from the 2028 close encounter with Earth.
- The evolution of orbital uncertainty caused by initial velocity increment errors is dominated by orbital phase.
- The timing of kinetic impact is found to significantly affect the subsequent uncertainty evolution of 2024 YR4.

中图分类号：V448.2 文献标识码：A 文章编号：2096-9287(2026)03-0287-12

DOI:10.3724/j.issn.2096-9287.2026.20250099

Reference format: YANG X M，ZHANG J Y，ZHANG F，et al. Analysis of deflection effect of 2024 YR4 asteroid under the velocity increment deviation of kinetic impact[J]. Journal of Deep Space Exploration, 2026, 13 (3) : 287-298.

引用格式：杨小敏，张建英，张烽，等. 动能撞击状态不确定性下的2024 YR4小行星偏转效果分析[J]. 深空探测学报（中英文），2026，13（3）：287-298.

Introduction

The discovery of near-Earth asteroid 2024 YR4 and the high-impact probability warning it triggered[1-2] underscore the urgency of developing reliable asteroid defense technologies. Among the various defense options, kinetic impact is considered one of the most feasible approaches due to its high level of technological maturity[3-4]. In 2021, NASA's Double Asteroid Redirection Test (DART) mission successfully demonstrated the kinetic impact technique, altering the orbital period of the binary asteroid system Dimorphos by 33 minutes[5-6], thereby validating the effectiveness of this technology.

Received：2025-08-13 Revised：2026-03-10

Fund program：National Research Special Project (No.KJSP2023020304), The Beijing Institute of Technology Research Fund Program for Young Scholars (Grant No.XSQD-202101012)

Previous research has established a theoretical framework for the deflection of asteroids through kinetic impactors within a two-body gravitational system. Vasile et al. derived an analytical expression for calculating the offset distance of an asteroid using Gauss's planetary equations[7]. Their study shows that the post-impact offset distance is closely related to the instantaneous direction of the velocity change imparted to the asteroid by the impact. In actual impact missions, the direction of the velocity increment delivered by the impactor to the asteroid is difficult to align perfectly with the theoretically optimal direction. This is due to various uncertainties associated with both the impactor and the asteroid. For the impactor, uncertainties include limitations in navigation accuracy, which can cause errors in its approach direction, impact angle, and impact point. For example, during the DART impact mission, the actual impact point deviated by approximately 25 meters from the originally intended target point[8]. Such random impact deviations inevitably affect the actual deflection outcome.

For the asteroid, its irregular shape and non-uniform mass distribution can cause significant perturbations to spacecraft operations in its vicinity, affecting the actual impact outcome. Furthermore, many asteroids (such as Bennu[9-10]) belong to loosely aggregated "rubble pile" structures. This type of structure undergoes complex processes of energy absorption and transfer upon impact[11]. Characteristics such as the internal porosity and boulder distribution of rubble-pile asteroids are difficult to model accurately, thereby limiting researchers' ability to predict the actual impact effects[12]. All the factors mentioned above can lead to discrepancies between the actual velocity increment imparted to the asteroid and the expected one. Minor errors at the moment of impact may result in significant deviations over the long-term orbital evolution process. Therefore, it is necessary to incorporate the uncertainties during the impact process into the research scope to accurately analyze the orbital evolution[13].

This paper addresses the kinetic impact defense problem for near-Earth asteroid 2024 YR4, establishing a high-precision orbital model that incorporates planetary perturbations and impact uncertainties, and systematically analyzes its deflection effectiveness. Section 1 introduces the dynamical model for orbit calculation, a semi-analytical method based on the State Transition Tensor (STT), and designs the generation method for velocity increment direction errors. Section 2 analyzes the orbital characteristics of 2024 YR4, identifying the 2032 close-approach window and the critical 2028 Earth encounter event, and calculates the theoretical maximum offset distances for different impact times using the theoretical model. Section 3 is the core analysis: it first demonstrates the effectiveness of the STT method for analyzing impact deflection problems; it then reveals that planetary perturbations, especially the 2028 Earth encounter event, cause the actual deflection distance to be lower than the theoretical value. Finally, it clarifies that the orbital phase dominates the error propagation pattern, while the magnitude of the velocity increment only affects the error amplitude. Section 4 summarizes the mechanisms by which planetary perturbations weaken the theoretical model and the laws of error propagation, providing theoretical support for defense mission design.

1 Asteroid deflection analysis method based on state transition tensor

1.1 Dynamics model

For the orbital evolution dynamics model of asteroids, this paper takes into account the gravitational perturbations of the eight planets in the solar system as well as that of the Moon. The expression is as follows

$$\frac{\mathrm{d}^2\boldsymbol{r}}{\mathrm{d}t^2}=-\frac{\mu_{\mathrm{s}}}{|\boldsymbol{r}|^3}\boldsymbol{r}-\sum_{i=1}^{8}\mu_{pi}\left(\frac{1}{\left|\boldsymbol{d}_{pi}\right|^3}\boldsymbol{d}_{pi}+\frac{1}{\left|\boldsymbol{\rho}_{pi}\right|^3}\boldsymbol{\rho}_{pi}\right)+a_{\mathrm{moon}} \quad (1)$$

where, $\boldsymbol{d}_{pi}$ represents the heliocentric vector of the i-th planet, and $\boldsymbol{\rho}_{pi}$ represents the vector from the i-th planet to the asteroid. The planetary and lunar star calendars use the DE432t star catalog to obtain the high-precision position data of the perturbing celestial bodies at each moment.

1.2 State transition tensor

After an asteroid is subjected to a kinetic impact, its actual trajectory will deviate from the original nominal orbit. Within the framework of this study, we consider the asteroid impact event as an instantaneous process[14]. Based on this premise, it can be assumed that the position vector of the asteroid remains unchanged at the time of the impact, while only the velocity vector undergoes a sudden change[15]. For this specific scenario, when the motion state

of the asteroid deviates from the nominal state, we can approximate the trajectory evolution process after the impact by applying the Taylor series expansion of the solution function to the initial conditions[16]. For a deviation of $\delta \boldsymbol{x}_0$, the approximate expression is

$$\delta \boldsymbol{x}^i(t) = \sum_{p=1}^{M} \frac{1}{p!} \underbrace{\boldsymbol{\Phi}_{(t,t_0)}^{i,k_1\cdots k_p}}_{\text{Higher-order transition tensor}} \delta \boldsymbol{x}_0^{k_1} \cdots \delta \boldsymbol{x}_0^{k_p} \tag{2}$$

Its derivative satisfies the following equation

$$\delta \dot{\boldsymbol{x}}^i(t) = \sum_{p=1}^{M} \frac{1}{p!} f^{i,k_1\cdots k_p} \delta \boldsymbol{x}^{k_1} \cdots \delta \boldsymbol{x}^{k_p} \tag{3}$$

where, i denotes the i-th component of the vector function, and M is the order of the Taylor series expansion. The State Transition Tensor (STT) is defined as

$$\boldsymbol{\Phi}_{(t,t_0)}^{i,k_1\cdots k_p} = \left. \frac{\partial^p x^i(t)}{\partial x_0^{k_1} \cdots \partial x_0^{k_p}} \right|_{x^i = \bar{x}_0^i} \tag{4}$$

These tensors relate the deviations in the initial conditions to the state deviations at a future time. The time derivative of the deviation $\delta \boldsymbol{x}^i$ can also be obtained by differentiating Equation (2)

$$\delta \dot{x}^i(t) = \sum_{p=1}^{K} \frac{1}{p!} \dot{\boldsymbol{\Phi}}_{(t,t_0)}^{i,k_1\cdots k_p} \delta x_0^{k_1} \cdots \delta x_0^{k_p} \tag{5}$$

In general, in the study of post-impact orbital evolution of asteroids, the order of the State Transition Tensor expansion is positively correlated with the prediction accuracy of the orbital error propagation model, but the computational complexity increases significantly as the order increases. Previous research has shown that in similar orbital deviation analyses, a second-order model can effectively balance accuracy requirements and computational efficiency. Therefore, for investigating the propagation of state errors following an asteroid impact, this paper likewise adopts a second-order accuracy model.

1.3　Theoretical optimal pulse direction calculation and error vector generation method

The theoretically optimal impulse direction is provided by an analytical model proposed by Vasile et al. This model derives a set of state transition matrices based on Gauss planetary equations and proximal motion equations[17-18]. The offset distance at the close-approach time can be obtained as a function of the velocity change $\delta \boldsymbol{v}(t_d)$ imparted to the asteroid at the impact time, with the relationship between them described by a three-step mapping mechanism

$$\delta \boldsymbol{v}(t_\mathrm{d}) \xrightarrow{\boldsymbol{G}_\mathrm{d}} \delta \boldsymbol{\alpha}(t_\mathrm{d}) \xrightarrow{\boldsymbol{A}_\mathrm{MOID}} \delta \boldsymbol{r}(t_\mathrm{MOID}) \tag{6}$$

$\boldsymbol{G}_\mathrm{d}$ is the state transition matrix that converts the velocity change $\delta \boldsymbol{v}(t_\mathrm{d})$ into changes in the orbital elements $\delta \boldsymbol{\alpha}(t_\mathrm{d})$. The period from the moment the spacecraft applies the impulse maneuver to the asteroid until the original time of the asteroid's predicted collision with Earth is defined as the lead time $\Delta t = t_\mathrm{MOID} - t_\mathrm{d}$. Subsequently, the offset $\delta \boldsymbol{r}(t_\mathrm{MOID})$ is obtained through the state transition matrix $\boldsymbol{A}_\mathrm{MOID}$. The objective is to maximize the offset distance

$$\| \delta \boldsymbol{r}(t_\mathrm{MOID}) \| = \| \boldsymbol{A}_\mathrm{MOID} \boldsymbol{G}_\mathrm{d} \delta \boldsymbol{v}(t_\mathrm{d}) \| = \max(\boldsymbol{T} \delta \boldsymbol{v}(t_\mathrm{d})) \tag{7}$$

The quadratic form $\boldsymbol{T}^\mathrm{T}\boldsymbol{T}$ must be maximized by selecting an impulse vector $\delta \boldsymbol{v}(t_\mathrm{d})$ that is parallel to its eigenvector v corresponding to the maximum eigenvalue, yielding the optimal impulse vector $\delta \boldsymbol{v}_\mathrm{opt}$ for achieving the maximum offset distance.

We assume that the impactor collides with the asteroid along the nominal design direction. The actual velocity increment of the asteroid in the solar reference system will be consistent with the theoretical optimal direction value of the above model, as shown in Figure 1.

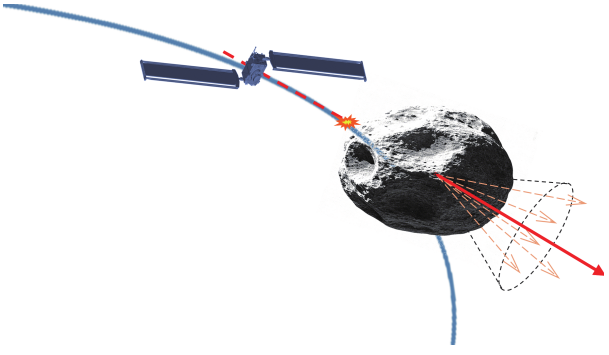


Fig. 1　Schematic diagram of velocity increment

However, the actual direction of the velocity increment will deviate from the nominal direction due to various uncertainties. First, the non-uniform internal composition of the asteroid (such as a mixed structure of a metallic core and a rubble-pile surface layer) can cause the mass and velocity distribution of the impact ejecta to deviate from the ideal model. Second, cumulative positioning errors in deep-space navigation and delays in

the spacecraft's maneuver response can cause the actual impact direction to deviate from the nominal axis. Although these complex physical and engineering factors are difficult to quantify precisely on an individual basis, their combined effects ultimately manifest as perturbations to the magnitude and direction of the velocity vector. Based on the superposition of the aforementioned error sources, this study constrains the impact direction within a conical range centered on the nominal direction.

We take the $\delta \boldsymbol{v}_{\text{opt}}$ direction as the reference direction, and generate candidate directions by superimposing three-dimensional normal distribution random perturbations on the central vector

$$x_{\text{cand}} = \delta \boldsymbol{v}_{\text{opt}} + \sigma \xi,\ \ \xi \sim N(\boldsymbol{0}, \boldsymbol{I}_3) \tag{8}$$

where σ represents the standard deviation (the σ in the following text refers to the standard deviation of the velocity increment direction perturbation), controlling the amplitude of the perturbation (the smaller the standard deviation, the more concentrated the direction), and ξ is isotropic Gaussian noise. Subsequently, the normalized candidate vectors $\boldsymbol{u}_{\text{cand}} = \boldsymbol{x}_{\text{cand}} / \|\boldsymbol{x}_{\text{cand}}\|$ are calculated. By calculating the angle between the candidate direction and the central vector, the directions that meet the conical constraint are selected

$$\cos\theta = \langle \boldsymbol{u}_{\text{cand}}, \boldsymbol{u}_{\text{center}} \rangle \geqslant \cos\theta_{\max} \tag{9}$$

where, $\theta_{\max}$ represents the conical angle, which is used to limit the maximum deviation range of the maximum speed increment.

We consider the calculated error scatter points to follow a multivariate Gaussian distribution $\mathcal{N}(\mu, \Sigma)$, and the covariance matrix Σ can be composed as

$$\boldsymbol{\Sigma} = \boldsymbol{Q}\boldsymbol{\Lambda}\boldsymbol{Q}^{\mathrm{T}},\ \ \boldsymbol{\Lambda} = \operatorname{diag}(\lambda_1, \lambda_2, \lambda_3) \tag{10}$$

where $\lambda_1 \geqslant \lambda_2 \geqslant \lambda_3 > 0$ is the eigenvalue and $\boldsymbol{Q} = [\boldsymbol{v}_1, \boldsymbol{v}_2, \boldsymbol{v}_3]$ is the eigenvector matrix. According to the properties of the multivariate normal distribution, the Mahalanobis distance $d^2 = (\boldsymbol{p}_i - \mu)^{\mathrm{T}} \Sigma^{-1} (\boldsymbol{p}_i - \mu)$ from a data point $\boldsymbol{p}_i$ to the mean $\boldsymbol{\mu}$ is defined as $d^2 = (\boldsymbol{p}_i - \mu)^{\mathrm{T}} \Sigma^{-1} (\boldsymbol{p}_i - \mu)$. The probability that the data point falls within the Mahalanobis distance range of 3σ is 99.7%. The boundary of this ellipsoid can be parameterized as

$$\mathcal{E}:\ \frac{(\boldsymbol{x}-\boldsymbol{\mu})^{\mathrm{T}}\boldsymbol{v}_1)^2}{a^2} + \frac{(\boldsymbol{x}-\boldsymbol{\mu})^{\mathrm{T}}\boldsymbol{v}_2)^2}{b^2} + \frac{(\boldsymbol{x}-\boldsymbol{\mu})^{\mathrm{T}}\boldsymbol{v}_3)^2}{c^2} = 1 \tag{11}$$

the length of the half shaft is obtained by scaling the square root of the characteristic value: $a = 3\sqrt{\lambda_1}, b = 3\sqrt{\lambda_2}, c = 3\sqrt{\lambda_3}$。

2 2024 YR4 Asteroid Natural Evolution Orbit Analysis

Asteroid 2024 YR4 is a near-Earth Apollo-type Potentially Hazardous Object (PHO). It was discovered by the Asteroid Terrestrial-impact Last Alert System (ATLAS) on December 27, 2024[19]. Its orbital dynamical parameters correspond to the epoch of May 5.0, 2025 (Ephemeris Time: 799,675,268). The asteroid's orbital semimajor axis is 2.516 astronomical units (AU), and its orbital eccentricity is relatively high at 0.662. Consequently, the difference between its perihelion and aphelion distances is significant, measuring 0.852 AU and 4.180 AU, respectively. Its orbital inclination is relatively low at 3.408°. The longitude of the ascending node and the argument of perihelion are 271.366° and 134.361°, respectively[20].

Based on the available observational data, we first computed the variation in the distance between 2024 YR4 and Earth over time, as shown in Figure 2. The gray curve in Figure 2(a) depicts the evolution of the distance between 2024 YR4 and Earth from May 5, 2025, to December 23, 2032, revealing a periodic oscillatory pattern in the spatial separation. The results indicate that the asteroid reaches its minimum distance to Earth on December 23, 2032, approximately 303,400 km (0.002 028 AU), corresponding to the end point of the curve. On December 22, 2032, it reaches its minimum distance to the Moon, about 48,300 km (0.000 32 AU), a value significantly less than the average Earth-Moon distance (approximately 384,000 km). Prior to this moment, the asteroid will experience a close approach to Earth on December 17, 2028, with a minimum distance of 0.053 73 AU, as indicated by the orange dashed line in the figure. During this close approach event, the orbital separation between the asteroid and Earth will enter a new observational window. This implies that within this timeframe, researchers can acquire new observational data to calibrate and refine the orbital information. Furthermore, during the 2028 close approach, the combined gravitational perturbation from Earth and the Moon will influence the subsequent trajectory of 2024 YR4.

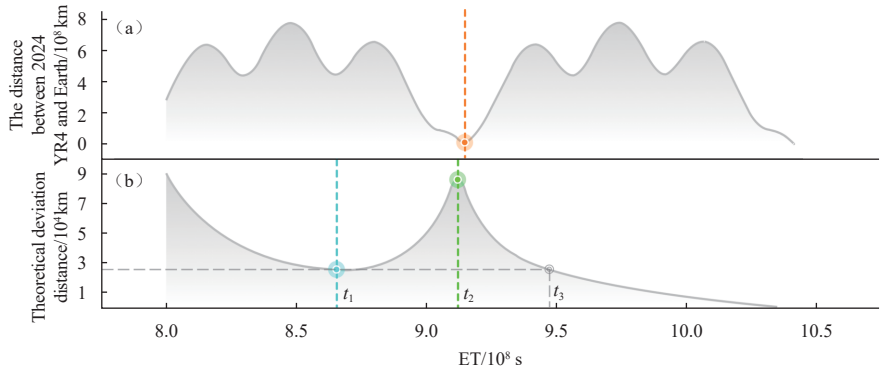


Fig. 2　Evolution of distance between 2024 YR4 and Earth over time (a) and Theoretical expected shift distance based on analytic model(b)

The gray curve in Figure 2(b) represents the theoretical offset distances corresponding to impacts at different times along the optimal impulse direction, based on the analytical model proposed by Vasile et al. This system quantifies the deflection effectiveness of kinetic impacts implemented during different time windows, with the theoretical offset distance curve exhibiting a nonlinear trend. To intuitively illustrate the relative positional relationship between Earth and the asteroid, this paper illustrates the evolution of the asteroid's position vector coordinates X and Y with Ephemeris Time (ET), as shown in the main plot on the left side of Figure 3. The blue and red curves represent the evolution of the X and Y coordinates of Earth and 2024 YR4's orbits over time, respectively. The leftmost starting point corresponds to the epoch of the observed orbital elements, and the rightmost endpoint corresponds to the time of the closest approach between the asteroid and Earth in 2032. Color planes perpendicular to the time axis mark three key orbital events. The blue plane indicates the potential impact time for the minimum theoretical offset distance (May 30, 2027, corresponding to the blue dashed line in Figure 2(b)). The green plane marks the impact time for the maximum theoretical offset distance (November 22, 2028, corresponding to the green dashed line in Figure 2(b)). The orange plane indicates the time of the close approach between the two bodies on December 17, 2028 (corresponding to the orange dashed line in Figure 2(a)).

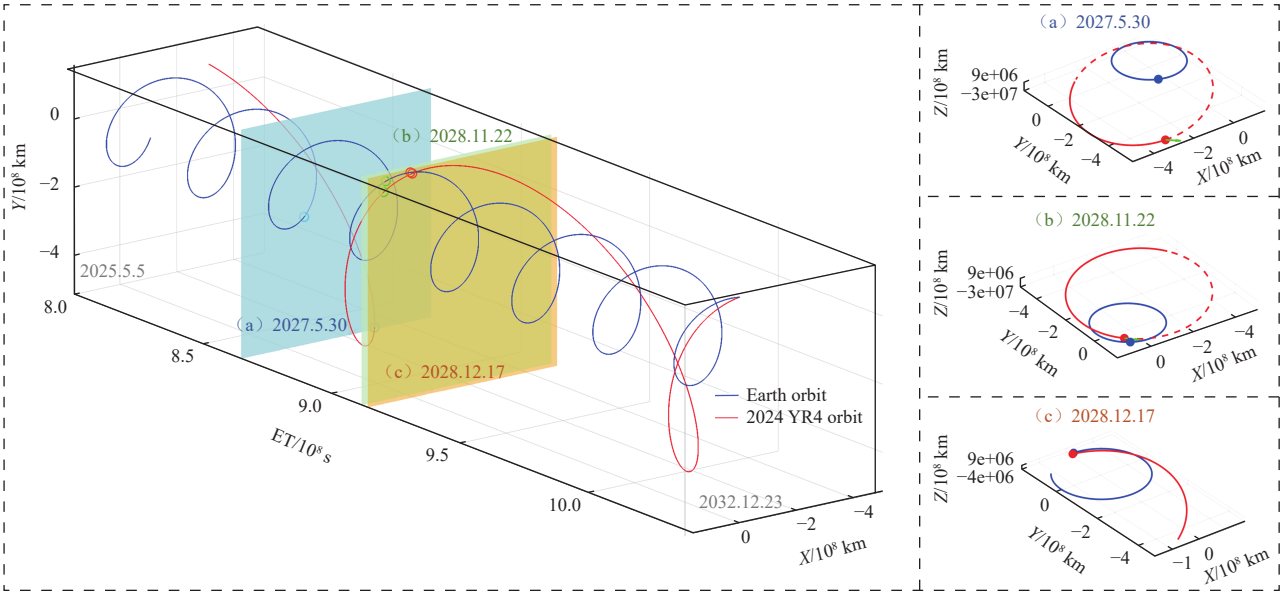


Fig. 3　Evolution of spatial configuration between Earth and asteroid 2024 YR4

The three subplots on the right side of Figure 3 correspond to the three key moments marked by the colored planes in the main plot, respectively, illustrating the spatial positional relationships between Earth and 2024

YR4 at those corresponding times. The red and blue dots in the figures represent the spatial positions of the asteroid and Earth at that moment, respectively. Figure 3(a) shows the positions of the celestial bodies at the impact time corresponding to the minimum offset distance: 2024 YR4 is near the aphelion of its orbit, with a significant separation from Earth. Figure 3(b) displays the relative positions of Earth and the asteroid at the impact time corresponding to the maximum offset distance, where the asteroid is near the perihelion of its orbit and the distance between the two is relatively small. Figure 3(c) presents the spatial positions at the time of the close approach between the asteroid and Earth.

3 Analysis of Orbital Deviation Considering Errors

3.1 Comparison of STT method with Monte Carlo results

To verify the reliability of the STT method in predicting and evaluating asteroid orbital deflection via kinetic impact, this section systematically compares the deviations between the results from Monte Carlo (MC) simulations based on high-precision numerical orbit propagation and those obtained from the semi-analytical STT method. The critical moment t_1, marked by the blue dashed line in Figure 2(b), is selected as the impact time. An impulse maneuver along the direction of velocity change $\delta \boldsymbol{v}_{\text{opt}}$ is applied at this moment. To simulate uncertainties, errors in the velocity increment magnitude of ±10% and a velocity increment direction error of σ=0.1 are introduced. Based on this error criterion, a random set containing 1,000 independent samples is generated for computation. Starting from time t_1, the orbits are propagated backward for 100, 500, 1 000, 1 500, and 2 000 days respectively to evaluate the evolution of the prediction results. The quantitative comparison of the errors is shown in Figure 4. The blue scatter points in the figure represent the relative error between the length of the 3σ envelope ellipsoid's major axis derived by the STT method and the corresponding MC result at each propagation time point. The red scatter points represent the absolute error between the 3σ envelope ellipsoid major axis lengths obtained by the STT and MC methods at each propagation time point.

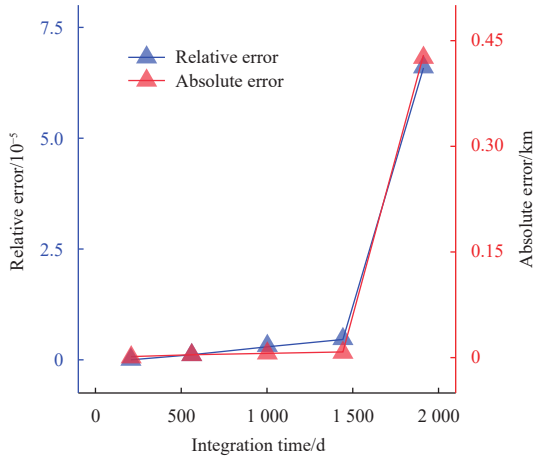


Fig. 4 Variation of absolute and relative errors along major axis of 3σ position error ellipsoid versus orbital propagation time

Figure 4 shows the distribution comparison and error evolution of the two result sets in three-dimensional position space. Within the time range of 0-1 500 days, both the relative error (blue line in the figure) and the absolute error (red line in the figure) of the major axis of the 3σ envelope ellipsoid exhibit a gentle growth trend. The relative error consistently remains below 4.69×10^{-6}, and the absolute error consistently stays below 7.6×10^{-3} km. When the propagation duration increases from 1 500 to 2 000 days, the absolute error rises to 0.425 1 km. The relative error increases correspondingly to about 7.5×10^{-6} (peak value of the blue line in the figure). Moreover, even with a propagation duration of 2 000 days, the maximum relative error remains within 7.5×10^{-6}, and the absolute error does not exceed 0.43 km. This level of accuracy meets the requirements of this study for analyzing the deflection effects of kinetic impact.

Figure 5 presents the simulated spatial distribution of orbital position uncertainty for the target asteroid after 2 000 days of propagation following a kinetic impact. In the figure, the blue circular scatter points represent the position samples calculated based on the State Transition Tensor (STT) method, while the red cross-shaped scatter points correspond to the results from the Monte Carlo (MC) simulation. It can be observed that the computational results from both methods are concentrated on the surface of an ellipsoid (depicted by the gray-white grid lines in the figure). A comparison reveals that the distribution contours of the blue and red point clusters in three-dimensional space are highly consistent, exhibiting nearly identical spatial configurations and distribution characteristics.

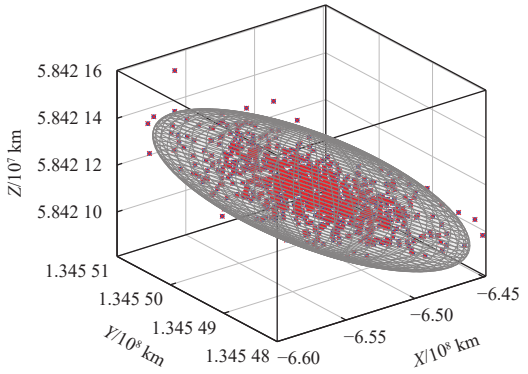


Fig. 5　Comparison of Monte Carlo results and STT results

3.2　Analysis of orbital element

The analytical model proposed by Vasile et al. is derived based on two-body dynamics and does not account for the perturbative effects present during actual orbital evolution. In this study, along the optimal impulse direction determined by their analytical model, precise numerical integration of the deflected orbit is performed by incorporating the gravitational perturbations from multiple planets and the Moon. To assess the comprehensive influence of planetary perturbations on the deflection effect, deflection calculations for the asteroid are conducted in this section at ten-day intervals. The distance between the deflected asteroid orbit and the unperturbed orbital position at the same epoch is recorded as the deflection distance, δr_S. Figure 6(a) compares the theoretically predicted offset distance δr_T (blue solid line) with the mean deflection distance δr_S (gray scatter points) calculated for specific target epochs. The simulation results, δr_S, are consistently lower than the theoretical results, δr_T, to varying degrees throughout the entire observation time window. This indicates that planetary perturbations have a diminishing effect on the deflection distance of asteroid 2024 YR4's orbit. Figure 6(b) quantitatively illustrates the temporal variation of the difference between δr_T and δr_S (blue dashed line). This curve reveals a three-stage pattern of discrepancy: Over a longer period before the time corresponding to the theoretical maximum of the deflection curve (around 9.5E+08 seconds in the figure), the theoretical value δr_T is higher than the simulated value δr_S (i.e., (δr_T - δr_S) is a relatively large positive value). As it approaches the aforementioned time of the theoretical maximum, the difference (δr_T - δr_S) reaches a local minimum, indicating that the theoretical prediction and simulation results are relatively closest near this point. After the time of the theoretical maximum, the difference (δr_T - δr_S) undergoes a slow increase before finally tending towards zero. This suggests that for impact times that are sufficiently late (closer to Earth), the theoretical results of the Vasile model converge with the simulation results that account for gravitational perturbations.

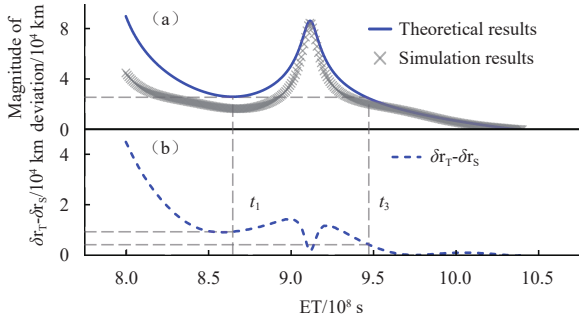


Fig. 6　Comparison between theoretical expected offset and actual offset results

To investigate the causes of the discrepancy between theoretical predictions and actual simulation results, this paper selects two typical impact times, t_1 and t_3, from Figure 2(b) for in-depth analysis. Both times share the same theoretical deflection distance but exhibit significant differences in numerical results. Specifically, time t_1 corresponds to the local minimum of the theoretical deflection distance within the studied time domain, while t_3 is another impact time that shares the same theoretical deflection distance as t_1. As shown in Figure 6, although the theoretical deflection distances are identical at these two times, the corresponding simulated deflection distances differ by approximately 4 000 km. To reveal the dynamical origin of this difference, we compared and analyzed the evolution characteristics of the asteroid's orbital elements after kinetic impacts at times t_1 and t_3 against its natural (non-impact) orbital evolution.

Specifically, the differential evolution curves of the three key orbital parameters (semimajor axis, eccentricity, and ascending node right ascension) relative to their natural evolution (without impact) reference values were calculated and plotted, as shown in Figure 7. It can be seen that the red curves in the three data sets remain at zero before time t_1. After time t_1, due to the application of an instantaneous velocity increment, the orbital elements

undergo an abrupt change. Both the impact at time t_1 (red solid line) and the impact at time t_3 (blue dashed line) induce abrupt changes in the orbital elements at their respective impact times, resulting from the instantaneous δv impulse applied during the impact. After the impact at time t_1, the red curve remains relatively constant for a considerable period, indicating that the dynamical environment is relatively stable when distant from major gravitational perturbations, and orbital elements are less prone to significant changes. A key difference emerges around November 22, 2028 (marked by the orange dashed line in the figure), which is the critical moment of close approach between Earth and the asteroid. Relative to the natural orbit, the difference in semimajor axis after the impact at time t_1 increases by approximately 100 km as the asteroid approaches Earth, and then decreases by about 350 km as it moves away. This substantial fluctuation reshapes the asteroid's orbital state. During the approach, the differences in eccentricity and right ascension of the ascending node also show a slight upward trend. The analysis above clearly indicates that it is precisely the strong gravitational perturbation induced by the close approach between Earth and the asteroid around November 22, 2028, that leads to significant changes in the orbital state. This event affects the asteroid's orbit after the impact at time t_1, causing the asteroid's trajectory to deviate substantially from its original path, ultimately resulting in an actual deflection effect that is lower than the theoretical prediction from the unperturbed model.

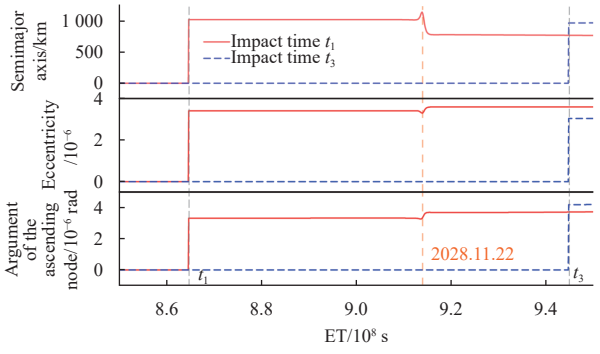


Fig. 7 Temporal variation of differences between post-impact and natural orbital elements at epochs t_1 and t_3

3.3 Error propagation analysis

In kinetic impact asteroid defense missions, the momentum transfer effect generated by the impactor hitting the target directly alters the orbital state of the asteroid. The uncertainty in the initial impact-induced velocity increment propagates and amplifies during subsequent orbital evolution. This section quantitatively analyzes the propagation of state uncertainty in asteroid 2024 YR4, caused by initial velocity increment errors, following a kinetic impact. For each impact time, 1,000 orbital velocity vectors incorporating velocity increment perturbations are generated, and the propagation of error effects is calculated using the State Transition Tensor. The evolution characteristics of the three-sigma envelope ellipsoid morphology for both the position and velocity vectors are analyzed, with the ellipsoid's major axis used to quantify the evolution of uncertainty. Figure 8 illustrates the dynamic evolution of the logarithm of the three-sigma envelope ellipsoid major axis for the position and velocity vectors as a function of orbital phase, with the horizontal coordinate representing the cumulative change in true anomaly.

Figure 8(a) illustrates the evolution pattern of position vector uncertainty. The variation in the major axis length of the 3σ error ellipsoid for the position vector under different δv magnitudes is presented on a logarithmic

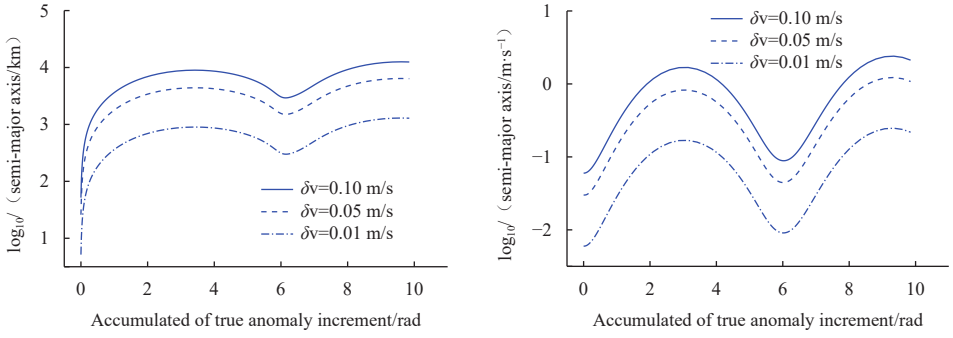


Fig. 8 Temporal evolution of major axis for 3σ position vector error ellipsoid(left) and Temporal evolution of major axis for 3σ velocity vector error ellipsoid(right)

scale. It can be observed that shortly after the kinetic impact, the orbital uncertainty increases sharply. Subsequently, the major axis of the envelope ellipsoid experiences a relatively gentle period of growth before entering a declining phase, eventually tending to rise again. Although the amplitudes of the three curves differ significantly—with the dotted blue line corresponding to δv=0.01 m/s having the lowest amplitude, and the solid line corresponding to δv=0.1 m/s having the highest—their overall evolutionary trends are highly consistent. This indicates that the orbital phase dominates the growth pattern of position uncertainty. Figure 8(b) shows the evolution of velocity vector uncertainty, displaying the variation in the major axis length of the 3σ error ellipsoid for the velocity vector on a logarithmic scale. Unlike the position vector, the velocity uncertainty does not exhibit the same dramatic initial surge seen in the position vector immediately after the impact. However, its subsequent evolutionary path similarly reveals a three-stage pattern of growth-decline-rise. Here too, the dotted line for δv=0.01 m/s has the lowest amplitude, and the solid line for δv=0.1 m/s has the highest. Regardless of whether for the position or velocity vectors, under different magnitudes of velocity increment, the variation trends of their respective 3σ ellipsoid major axes are highly consistent. This demonstrates that the initial velocity increment (δv) introduced by the error primarily determines the scale of the propagated position and velocity uncertainties, while the orbit dynamics itself (reflected in the orbital phase evolution via the change in true anomaly) govern the temporal pattern of this uncertainty evolution. To systematically analyze the influence of the kinetic impact timing on orbital uncertainty, this paper separately examines the evolution of orbital position vector errors for the impact time points t_1 and t_2 marked in Figure 2(b). As shown in Figures 9 and 10, the two figures correspond to the schematic diagrams of error evolution for kinetic impact time t_1 and t_2, respectively. In the main orbital diagram on the left side of each figure, the impact time is marked, and the orange plane indicates the time point corresponding to the close approach between 2024 YR4 and Earth in 2028. The planes labeled (a) through (d) in the figures represent the epochs corresponding to 100 days, 500 days, 1 000 days, and the close approach in 2032, respectively, of orbital propagation backward from the impact time. Furthermore, the three-dimensional error ellipsoid at the epoch corresponding to each time plane is plotted.

In the case of an impact occurring at time t_1, the position error ellipsoid rapidly expands after a short-term evolution of 100 days, with the major axis length reaching 260.3 km (Figure 9(a)). Furthermore, the lengths of the

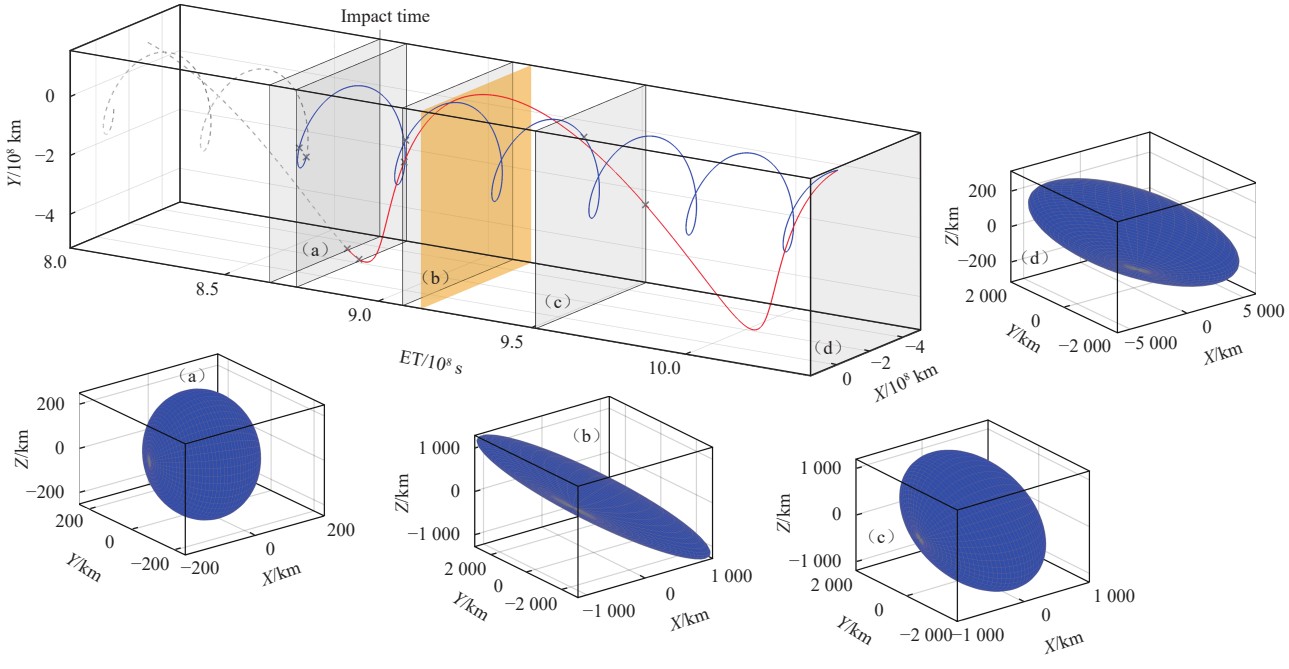


Fig. 9　Temporal evolution of orbital position errors after impact at epoch t_1

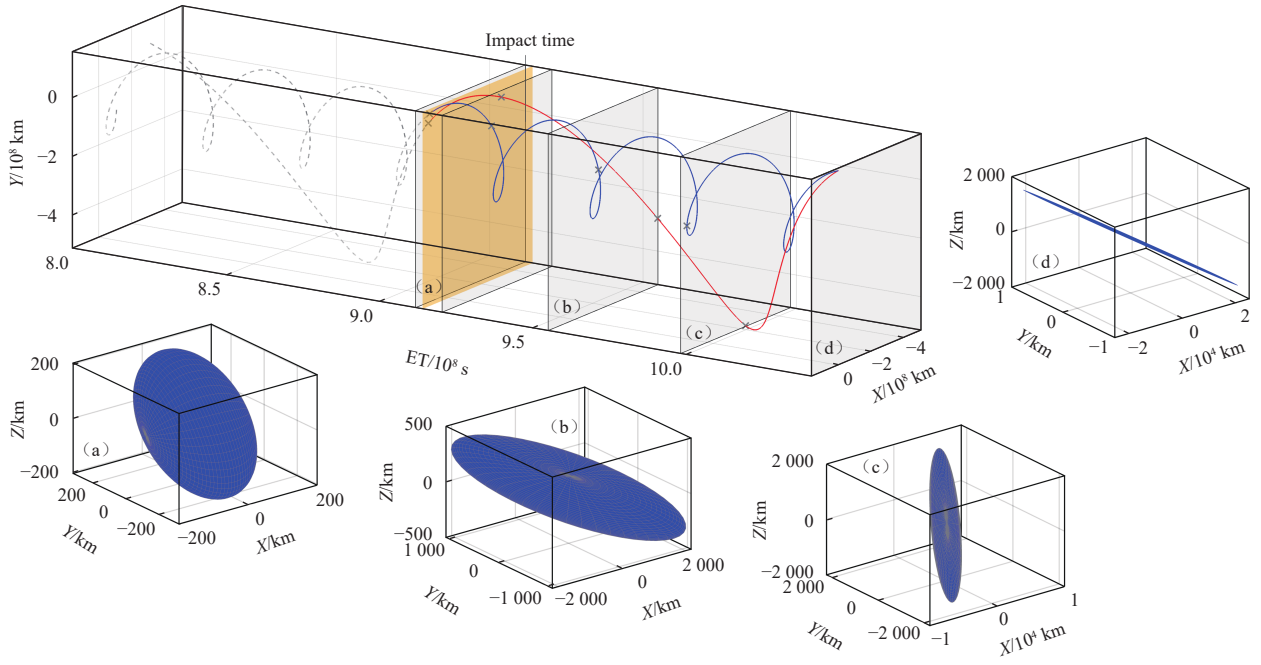


Fig. 10 Temporal evolution of orbital position errors after impact at epoch t_2

three axes of the ellipsoid are nearly equal, and its shape approximates a sphere, indicating that the error propagation at this stage exhibits isotropic characteristics. In contrast, for an impact at time t_2, the error ellipsoid after the same short-term evolution exhibits a larger major axis length of 341.4 km (Figure 10(a)). This demonstrates that the propagation of orbital uncertainty does not increase uniformly with evolution time but is also related to the orbital phase at the moment of impact. By 1 000 days after the impact, as evolution time progresses, the error ellipsoids for both impact times undergo significant deformation and pronounced elongation along a single direction. In the case of the t_1 impact, the major axis grows to 1,988 km (Figure 9(c)), while for the t_2 impact, it increases to 7,289 km (Figure 10(c))—3.7 times that of the former. By the end of the calculation period, the difference in error scale between the t_1 and t_2 cases becomes more pronounced. The major axis of the ellipsoid for the t_1 case expands to 6,276 km, whereas for the t_2 impact time, it inflates to 26,526 km (Figure 10(d)), exceeding 4.2 times the major axis length for the t_1 case. This indicates that between the two kinetic impact times, t_1 and t_2, the impact performed at the time with the larger theoretical offset (t_2) results in a longer major axis of the 3σ envelope ellipsoid for the position vector by the end of the calculation period.

4 Conclusion

The kinetic impact method alters an asteroid's trajectory through momentum transfer generated by instantaneous collision and is currently the most effective means of planetary defense. Using asteroid 2024 YR4 as a case study, this paper employed the State Transition Tensor (STT) method to analyze the asteroid orbital impact problem under uncertainty. Subsequently, by comparing the orbital evolution for two impact times that share the same theoretically predicted offset distance, the reasons for the discrepancy between the theoretical and actual offset results were investigated. Finally, the error propagation patterns were analyzed by comparing the variations in the major axis of the orbital error ellipsoid after impact deflection.

(1) By analyzing the evolution of orbital elements after impacts at different times, the study found that the strong gravitational perturbations experienced by asteroid 2024 YR4 during its close approach to Earth are the fundamental cause for the actual post-impact orbital offset being smaller than the theoretical prediction. This gravitational interaction dynamically reshapes the orbital elements, causing the orbital phase change intended to be induced by the impact to be partially counteracted, ultimately manifesting as an attenuation of the actual deflection effect.

(2) In kinetic impact asteroid defense missions, the uncertainty in the initial impact-induced velocity increment (δv) is amplified and propagates during subsequent orbital evolution. Quantitative analysis of asteroid 2024 YR4 indicates that the major axes of the 3σ envelope ellipsoids for the position and velocity vectors do not increase monotonically with evolution time but exhibit a certain degree of fluctuation. When impacts are applied at different initial times and propagated for the same duration, the difference in the major axis length of the error ellipsoid can reach 3.7 times, highlighting the significant influence of impact timing on the uncertainty of orbital deflection effectiveness. Different δv magnitudes (0.01 m/s to 0.1 m/s) only affect the amplitude of the uncertainty, while the evolutionary patterns are highly consistent, indicating that orbital phase dynamics dominate the mode of uncertainty propagation.

References

[1] RIVKIN A S, MUELLER T, MACLENNAN E, et al. JWST observations of potentially hazardous asteroid 2024 YR4[J]. Research Notes of the AAS, 2025, 9(4): 70-76.

[2] SMIRNOV E A. Chaotic diffusion and transient resonance captures of the near-Earth asteroid 2024 YR4[J]. Astronomy & Astrophysics, 2025, 699: A26-34.

[3] THOMAS C A, Naidu S P, Scheirich P, et al. Orbital period change of Dimorphos due to the DART kinetic impact[J]. Nature, 2023, 616(7957): 448-451.

[4] ZHANG H, GU Z, ZHANG X Y, et al. Feasibility study on the defense of near Earth asteroids[J]. Sci Sin Tech, 2024, 54: 1435-1445.

[5] LI J Y, HIRABAYASHI M, FARNHAM T L, et al. Ejecta from the DART-produced active asteroid Dimorphos[J]. Nature, 2023, 616(7957): 452-456.

[6] DALY R T, ERNST C M, BARNOUIN O S, et al. Successful kinetic impact into an asteroid for planetary defence[J]. Nature, 2023, 616(7957): 443-447.

[7] CHENG A F, MICHEL P, JUTZI M, et al. Asteroid impact & deflection assessment mission: kinetic impactor[J]. Planetary and space science, 2016, 121: 27-35.

[8] FRANZESE S, BASILE E, POLLI E M, et al. Analysis of asteroid deflection mission options for the 2025 planetary defense conference hypothetical asteroid impact threat scenario by the italian space agency delegation at SMPAG[C]//Proceedings of 9th IAA Planetary Defense Conference (PDC 2025). [S. l.]: IAA, 2025: 1-18.

[9] VASILE M, COLOMBO C. Optimal impact strategies for asteroid deflection[J]. Journal of guidance, control, and dynamics, 2008, 31(4): 858-872.

[10] LI X, WARIER R R, SANYAL A K, et al. Trajectory tracking near small bodies using only attitude control[J]. Journal of Guidance, Control, and Dynamics, 2019, 42(1): 109-122.

[11] WALSH K J. Rubble pile asteroids[J]. Annual Review of Astronomy and Astrophysics, 2018, 56(1): 593-624.

[12] BARNOUIN O S, DALY M G, PALMER E E, et al. Shape of (101955) Bennu indicative of a rubble pile with internal stiffness[J]. Nature geoscience, 2019, 12(4): 247-252.

[13] DAI K, LUO X Z, ZHU M H, et al. Impact momentum transfer—insights from numerical simulation of impacts on large boulders of asteroids[J]. The Planetary Science Journal, 2024, 5(9): 214-220.

[14] HERBST W, GREENWOOD J P, YAP T E. The macroporosity of rubble pile asteroid Ryugu and implications for the origin of chondrules[J]. The Planetary Science Journal, 2021, 2(3): 110-119.

[15] CHEN Y Y, HU S C, LI X R, et al. Specific application of planetary orbital dynamics on deflection method of kinetic impact[J]. Space Debris Research, 2022, 22(3): 46-59.

[16] SCHAUB H, JUNKINS J L. Analytical mechanics of space systems[M]. USA: AIAA, 2003.

[17] BATTIN R H. An introduction to the mathematics and methods of astrodynamics[M]. USA: AIAA, 1999.

[18] PARK R S, SCHEERES D J. Nonlinear mapping of Gaussian statistics: theory and applications to spacecraft trajectory design[J]. Journal of guidance, Control, and Dynamics, 2006, 29(6): 1367-1375.

[19] FARNOCCHIA D, FENUCCI M, BERNARDI F, et al. The impact hazard assessment for near-Earth asteroid 2024 YR4[J]. The Journal of the Astronautical Sciences, 2026, 73(2): 28-35.

[20] BOLIN B T, HANUŠ J, DENNEAU L, et al. The discovery and characterization of Earth-crossing asteroid 2024 YR4[J]. The Astrophysical Journal Letters, 2025, 984(1): L25-32.

The Author Profiles

YANG Xiaomin(1997−), male, Ph.D. candidate. Main research direction: asteroid impact defense.

Address: School of Aerospace Engineering, Beijing Institute of Technology, Beijing 100081, China

E-mail: yang_x.m@qq.com

LI Xiangyu(1991−), male, associate professor, Ph.D supervisor. Main research direction: asteroid detection dynamics. **Corresponding Author**.

Address: School of Aerospace Engineering, Beijing Institute of Technology, Beijing 100081, China

E-mail: lixiangy@bit.edu.cn

动能撞击状态不确定性下的2024 YR4小行星偏转效果分析

杨小敏[1]，张建英[2]，张　烽[2]，李翔宇[1]

（1. 北京理工大学 空天科学与技术学院，北京 100081；
2. 中国运载火箭技术研究院，北京 100076）

摘　要：本文针对近地小行星2024 YR4的动能撞击防御问题，研究了速度增量偏差下的轨道偏转效果。首先，建立了融合行星摄动与撞击误差的轨道演化模型；其次，通过状态转移张量（STT）半解析方法，系统分析了速度增量误差对小行星轨道偏转效果的影响；最后分析了在不同时刻进行撞击后的误差椭球长轴演化差异。研究发现，初始速度增量误差引发的轨道不确定性演化由轨道相位主导，速度增量的大小仅影响误差幅度而非传播形态。在选取不同初始时刻实施撞击，并演化相同时长的情况下，误差椭球长轴尺寸的差异可达3.7倍，这表明撞击时机对轨道偏转效果的不确定性具有重要影响。此外，分析发现2028年的地星交会事件将改变偏转预期。本研究为考虑误差传播的小行星防御策略制定提供了参考。

关键词：不确定性；小行星；动能撞击；状态转移张量

[责任编辑：高莎，英文审校：宋利辉]